

Article type:

Submitted version – Preprint

Full citation:

Claudio Palazzo, Giuseppe Trapani, Gilles Ponchel, Adriana Trapani, Christine Vauthier*. Mucoadhesive properties of low molecular weight chitosan- or glycol chitosan and corresponding thiomers-coated poly(isobutylcyanoacrylate) core-shell nanoparticles. *European Journal of Pharmaceutics and Biopharmaceutics* 117 (2017) 315–323, DOI: 10.1016/j.ejpb.2017.04.020.

Publication History:

Received 31 December 2016, available online 25 April 2017, version of Record 8 May 2017

Source name:

European Journal of Pharmaceutics and Biopharmaceutics

ISSN: 0939-6411

E- ISSN: 1873-3441

Editor:

Elsevier

Link for final version:

<https://www.sciencedirect.com/science/article/pii/S0939641116310517?pes=vor>

This is a submitted-preprint version of an accepted manuscript. Note that revisions and technical editing may introduce changes to the manuscript text and/or graphics which could affect content. To access to the final version click the link above.

Mucoadhesive properties of low molecular weight chitosan- or glycol chitosan- and corresponding thiomers-coated poly(isobutylcyanoacrylate) core-shell nanoparticles

Claudio Palazzo^{1,2*}, Giuseppe Trapani², Gilles Ponchel¹, Adriana Trapani², Christine Vauthier¹

¹Institut Galien Paris-Sud, CNRS, Univ. Paris-Sud, Université Paris-Saclay, 5 rue Jean-Baptiste Clément, 92290 Châtenay-Malabry, France

²Dipartimento di Farmacia-Scienze del Farmaco, Università degli Studi di Bari “Aldo Moro”, Via Orabona, 4 – 70125 Bari, Italy

*Corresponding author

e-mail: claudio.palazzo@ulg.ac.be

List of abbreviations

60		
61		
62		
63		
64		
65		
66	PACA	Poly(alkylcyanoacrylate)
67		
68	PIBCA	Poly(isobutyl cyanoacrylate)
69		
70	CS	Chitosan
71	CS-GSH	Chitosan Glutathione conjugate
72		
73	CS-NAC	Chitosan <i>N</i> -acetyl-cysteine conjugate
74	CSGSH-P-NPs	Chitosan glutathione coated poly(isobutyl cyanoacrylate)
75		nanoparticles
76		
77	CSNAC-P-NPs	Chitosan <i>N</i> -acetyl-cysteine coated poly(isobutyl cyanoacrylate)
78		nanoparticles
79		
80		
81	CS-P-NPs	Chitosan coated poly(isobutyl cyanoacrylate) nanoparticles
82	CS-TBA	Chitosan-4-thiol-butylamidine
83		
84	GCS	Glycol chitosan
85		
86	GCS-GSH	Glutathione conjugate
87	GCS-NAC	<i>N</i> -acetyl-cysteine conjugate
88		
89	GCS-GSH	Glycol Chitosan Glutathione conjugate
90	GCS-NAC	Glycol Chitosan <i>N</i> -acetyl-cysteine conjugate
91		
92	GCS-P-NPs	Glycol chitosan coated poly(isobutyl cyanoacrylate)
93		nanoparticles
94		
95	GCSNAC-P-NPs	Glycol chitosan <i>N</i> -acetyl-cysteine coated poly(isobutyl
96		cyanoacrylate) nanoparticles
97		
98	GCSGSH-P-NPs	Glycol chitosan glutathione coated poly(isobutyl cyanoacrylate)
99		nanoparticles
100		
101	Isc	Short-circuit current
102		
103	LMW	Low Molecular Weight
104		
105	M%/cm ²	The percentage of NPs stuck on 1 cm ² of the mucosal surface
106	NPs	nanoparticles
107		
108	PD	Transmucosal potential difference
109		
110	PDI	Polydispersity index
111	QELS	Quasi-elastic light scattering
112		
113	TEER	Transmucosal electrical resistance
114	TEM	Transmission electron microscopy
115		
116		
117		
118		

Abstract

The aim of the present work was to evaluate the mucoadhesive properties of poly(isobutyl cyanoacrylate) (PIBCA) nanoparticles (NPs) coated with Low Molecular Weight (LMW) chitosan (CS)- and glycol chitosan (GCS)-based thiomers as well as with the corresponding LMW unmodified polysaccharides. For this purpose, all the CS- and GCS-based thiomers were prepared under simple and mild conditions starting from the LMW unmodified polymers CS and GCS. The resulting NPs were of spherical shape with diameters ranging from 400 to 600 nm and 187 to 309 nm, for CS- and GCS-based NPs, respectively. The mucoadhesive characteristics of these core shell NPs were studied in Ussing chambers measuring the percentage of NPs stuck on the mucosal of fresh intestinal tissue after 2 h of incubation. Moreover, incubation of nanoparticle formulations with the intestinal tissue induced changes in transmucosal electrical resistance which were measured to gain information into the opening of tight junctions and to control the integrity of the mucosa. Thus, it was found that PIBCA NPs coated with the GCS–Glutathione conjugate (GCGPIBCA NPs) possessed the most favorable mucoadhesive performances. Moreover, both GCGPIBCA- and GCS-*N*-acetyl-cysteine (GCNPIBCA)-core-shell NPs might induced an enlargement of the epithelial cell tight junctions. In conclusion, coating of PIBCA NPs with GCS-based thiomers may be useful for improving the mucoadhesive and permeation properties of these nanocarriers.

Keywords: Mucoadhesion, Thiomers, Ussing chambers, Chitosan, Glycol Chitosan

Introduction

Mucoadhesive polymers have been extensively studied over the past of decades because they are able to interact with mucus and remain on mucosal tissue for extended period of time [1-4]. Therefore, associated drugs can efficiently accumulate in the mucus near absorption sites creating favorable conditions to enhance their absorption hence their bioavailability [5]. The physiological function of the mucus is to protect the underlying epithelia from the luminal content as well as to catch nutrients to be absorbed [6]. This viscous liquid is mainly constituted by glycoproteins (“mucins”) composed of a protein backbone in which carbohydrate chains are grafted. At the pH of the gut, these side chains are highly negatively charged.

Most of polymers that interact with mucins found in the gut are hydrophilic and positively charged in the gut environment. Among these, chitosan (poly[β -(1-4)-2-amino-2-deoxy-D-glucopyranose]) (CS) is a cationic polysaccharide obtained by deacetylation of chitin, which is the most abundant polysaccharide in nature, after the cellulose. CS is a hydrophilic, biodegradable and biocompatible polymer that possesses hydroxyl and amine groups that can give rise to hydrogen bonding-mediated interactions with components of the mucus. These properties together with the polycationic nature, make the CS a good mucoadhesive polymer [7]. In fact, the positive charges on the chain of CS can interact with sialic and sulfonic acids of the mucus layer through strong electrostatic interactions. In general, the solubility of CS is rather poor in aqueous media including biological fluids. Various strategies were developed to increase the solubility of CS in these media. For instance, glycol chitosan (GCS) that can be obtained adding hydrophilic ethylene glycol groups on CS, is a typical water soluble CS derivative at neutral and acidic pH [8-10]. Reducing the molecular weight of CS based on depolymerization reaction is another strategy that was proposed to improve the solubility of CS at neutral pH [11].

Mucoadhesive properties of CS can also be strongly enhanced incorporating free thiol groups in the polysaccharide structure. This can be done by grafting free thiol group containing molecules such as thioglycolic acid [12], 2-iminothiolane[13], thioethylamide [14], *N*-acetylcysteine (NAC) [15] or glutathione (GSH) [16] along the chitosan leading to a class of mucoadhesive polymers denoted as thiomers. For instance, the covalent attachment of thioglycolic acid and 2-iminothiolane improved the mucoadhesion of the corresponding thiomers by 10 and 140 times in comparison to the mucoadhesion shown by the parent chitosan. The mechanism that was proposed to explain the observed improvement in

237
238
239
240 mucoadhesion of the thiomers is based on the formation of disulfide bonds between thiol
241 groups of the thiomers and thiol groups of cysteine residues found on mucus glycoproteins
242 [17]. In addition to their mucoadhesive properties, chitosan derivatives including GCS-NAC
243 (400 kDa) and GCS (400 kDa) were reported to inhibit the activity of efflux pump proteins
244 like the P-gp occurring in most mucosal tissue including the gut [10, 18]. These efflux pumps
245 were identified to participate to the poor bioavailability of numerous drugs from oral dosage
246 [18]. In these cases, inhibition of the P-gp generally enhances drug absorption as reported
247 considering important anticancer agents such as Paclitaxel [19].

248
249 In previous studies, it has been shown that poly(alkylcyanoacrylate) (PACA) nanoparticles
250 (NPs) are able to encapsulate peptides, proteins [20-23] and anticancer agents [19]. However,
251 due to the hydrophobic character of PACA as well as to the polyanionic nature of the
252 corresponding NPs, their mucoadhesive potential is generally low and therefore they are of
253 limited usefulness for transmucosal delivery. The mucoadhesion of these NPs, was enhanced
254 coating them with CS and thiolated CS such as CS-4-thiol-butylamidine (CS-TBA) [24]. In
255 addition to an improved mucoadhesion that was attributed to the formation of disulfide bonds
256 between thiol groups of the thiomers and thiol groups found on mucin chains, a permeability
257 of the gut epithelium through the paracellular route was also reported [25]. In this context, it
258 appeared of interest to compare the fate and properties of different (thiomers-coated)
259 poly(isobutyl cyanoacrylate) (PIBCA) core-shell NPs on native fully functioning intestinal
260 mucosa. It with the aim to improve their drug delivery efficacy by the oral route. More
261 precisely, the designed coatings were constituted by Low Molecular Weight (LMW) chitosan
262 (CS)- and glycol chitosan (GCS)-based thiomers as well as by the corresponding LMW
263 unmodified polysaccharides taking into account the favorable effect on the solubility of CS at
264 neutral pH [11] due to the reduction of its molecular weight. In such a way not only GCS and
265 derived polymers but also the corresponding CS based polymers should be endowed with
266 adequate solubility at neutral and physiological conditions. Thus, our working hypothesis was
267 that these polymers could confer to the nanoparticles interesting mucoadhesive properties
268 with potential to increase mucoadhesion and permeability of the gut intestine in physiological
269 conditions.

280 281 282 **2. Materials and methods**

283 284 285 *2.1 Materials*

286
287
288
289
290
291
292
293
294
295

296
297
298
299 Chitosan (CS) (low molecular mass: 20 kDa; degree of deacetylation: 92%) was purchased
300 from Amicogen.inc (Jinju, South Korea). Glycol chitosan (GCS), *N*-acetyl-L-cysteine (NAC),
301 L-Glutathione reduced form (GSH), Rhodamine B, 1-ethyl-3-(3-dimethylaminopropyl)
302 carbodiimide hydrochloride (EDAC), *N*-Hydroxysuccinimide (NHS) were all purchased by
303 Sigma-Aldrich (St. Louis, MO, USA).
304
305
306

307 308 *2.2 Methods*

309 310 311 *2.2.1 Purification of chitosan*

312
313 One gram of CS was purified by dissolution in MilliQ[®] water (50 mL) and the mixture was
314 stirred at room temperature for 15 min. Then, the polymer solution was purified by dialysis
315 (molecular weight cutoff 3500 g/mol), twice (2 h, overnight) against 1L of 1 mM
316 hydrochloric acid solution .
317
318
319
320

321 322 *2.2.2 Depolymerization of glycol chitosan*

323 The depolymerization of GCS was developed following the procedure proposed by Knigh et
324 al. [26]. Briefly, 500 mg of GCS were dissolved in 12.5 mL of acetic acid solution (6% v/v)
325 and stirred for 2 h at room temperature in the presence of 2.5 mL of sodium nitrite solution
326 (11 g/L). The polymer solution was purified by dialysis in tubing (molecular weight cutoff
327 3500 g/mol), twice during 1 h and once overnight against 1 L of distilled water. After
328 purification, the purified reaction mixture was lyophilized using an Alpha 1-2 LD plus
329 lyophilizator (Bioblock Scientific instrument).
330
331
332
333
334

335 336 *2.3 Synthesis of chitosan and glycol chitosan conjugates*

337 The CS-conjugates with *N*-acetyl-L-cysteine (CSNAC) and L-Glutathione (CSGSH) were
338 obtained adapting the methods described by Bernkop-Schnürch *et al.* with CS at high
339 molecular weight (HMW) [15,16,18]. Briefly, to prepare CSNAC, 150 mg of CS were
340 dissolved in 10 mL of MilliQ[®] water. In another flask, 150 mg of NAC were dissolved in 10
341 mL of MilliQ[®] water. The carboxylic group of NAC was activated by addition of 1.37 mmol
342 of EDAC followed by 20 min reaction. Then, the two preparations were combined and stirred
343 at room temperature for 7 h.
344
345
346
347

348 The preparation of CSGSH was carried out following the above described procedure for
349 CSNAC with a little modification. The carboxylic group of GSH was activated by addition of
350
351
352
353
354

355
356
357
358 both EDAC (2.13 mmol) and NHS (1.78 mmol). The reaction was allowed to proceed for 20
359 min. Both CSNAC or CSGSH were purified by dialysis in tubing (molecular weight cutoff
360 3500 g/mol) at room temperature. The dialysis was performed with the following sequence of
361 counter dialyzing media: MilliQ® water for 24 h, EDTA (0.2 µM) solution for 24 h, and
362 MilliQ® water for 24 h. Purified CSGSH was recovered after freeze-drying of the dialysate
363 using an Alpha 1-2 LD plus lyophilizator (Bioblock Scientific instrument).
364
365
366
367 LMW-GCSNAC and -GCSGSH were prepared adapting the methods described by Trapani *et*
368 *al.* [10] for GCS at high molecular weight.
369
370

371 372 2. 4 Preparation of PIBCA nanoparticles

373
374 NPs were prepared according to the redox radical emulsion polymerization method
375 developed by Chauvierre *et al.* [27-29]. Briefly, the appropriate polysaccharide (130 mg) was
376 dissolved in HNO₃ 0.2 M (8 mL) at 42°C under vigorous stirring and argon atmosphere.
377 Once the dissolution was completed, ammonium cerium (IV) nitrate (8×10^{-2} M) in HNO₃ 0.2
378 M (2 mL) and IBCA (0.5 mL) were added, the argon flux was stopped and the reaction was
379 allowed to continue at 42°C for another 50 min. Then, the nanoparticle suspension was
380 purified by dialysis (cutoff 100.000 g/mol, Spectra/Por membranes) three times against HCl
381 at pH 2.54 for 1 h and once overnight. The suspensions of PIBCA NPs coated with CS (CS-
382 P-NPs), GCS (GCS-P-NPs), CSNAC (CSNAC-P-NPs), CSGSH (CSGSH-P-NPs), GCSNAC
383 (GCSNAC-P-NPs) and GCSGSH (GCSGSH-P-NPs) (Figure 1) were stored under argon
384 atmosphere until further use.
385
386
387
388
389
390

391 [Insert Figure 1]

392
393 The NPs were labeled with Rhodamine B as follows. Rhodamine B was dissolved in CH₃CN
394 to give a solution of 4 mg/mL and, together with IBCA, added to the mixture containing the
395 polysaccharide in HNO₃ above mentioned. The polymerization reaction in the presence of
396 Rhodamine B was carried out in the dark and working up as above mentioned, the required
397 labeled NPs were obtained.
398
399

400
401 All the NPs prepared were stored in HCl at pH 2.5, in absence of air and in dark vials in order
402 to avoid aggregation and oxidation of thiol groups of the modified chitosan.
403

404
405 Hydrodynamic mean diameter, *d*, and size distribution, PDI, of the NPs were determined by
406 quasi-elastic light scattering (QELS) using a Zetasizer Malvern SZ90 (Malvern Instrument,
407 Orsay, France) and fixing the scattered angle at 90°. Samples were diluted in MilliQ® water
408
409
410
411
412
413

414 until a concentration of 0.35 mg/mL. Results were expressed as the mean hydrodynamic
415 diameter, and polydispersity index (PDI) of the size distribution.
416

417 The ζ potential was deduced from the electrophoretic mobility of the particles measured by
418 Laser Doppler Electrophoresis (Zetasizer Malvern SZ90, Malvern Instrument, Orsay, France)
419 in a NaCl solution (1 mM) after suitable dilutions (1/100 (v/v)) of the different nanoparticle
420 suspensions. The ζ potentials were evaluated at two pH values *i.e.*, 2.5 and 7.0.
421
422
423
424
425
426

427 *2. 5. Morphology of the nanoparticles*

428 The morphology of the NPs was investigated by transmission electron microscopy (TEM).
429 The nanoparticle aqueous dispersion (50 μ L) was dropped on the grid and left to dry. Then
430 nanoparticles were stained with a solution of phosphotungstic acid at 1% (pH 7.3) for 5
431 minutes. Electron micrographs were acquired using an electron microscope JEOL 1400 MET
432 operating at 80 kV (Electron Microscopy Facility of I2BC, CNRS, Gif sur Yvette, France,
433 <http://www.cgm.cnrs-gif.fr/spip.php?article282&lang=fr>) equipped with a high-resolution
434 digital CCD Gatan digital camera (11 megapixels). The nanoparticles were characterized by
435 measuring their long and short axis.
436
437
438
439
440
441
442
443

444 *2. 6 . Quantification of thiol groups content by iodometric titration*

445 The total amount of SH-groups of CS- and GCS-P-NPs was measured by iodometric titration
446 [24,30]. Briefly, an aliquot of NPs dispersion (2.5 mL) was incubated with 250 μ L of acetate
447 buffer (pH 2.7), 300 μ l of a solution of iodine (1 mmol/L) and 500 μ L of a solution of starch
448 (4 %). The iodine solution was prepared at 0.1 M concentration by dissolving 0.63 g of I₂ and
449 1.93 g of KI in 25 mL of MilliQ[®] water, stored protected from light and diluted before the
450 assay. The mixture was left at room temperature for 24 h protected from light. Then, the
451 samples were ultra-centrifuged (15 min, 30,000 rpm) to allow the sedimentation of NPs and
452 the absorbance of the supernatant was measured at a wavelength of 570 nm. The amount of
453 thiol groups was calculated from the calibration curve obtained using solutions of cysteine-
454 HCl at known concentrations (20-70 mmol/L). Iodine promotes the oxidation of thiol groups,
455 while the excess of iodine reacts with starch to form a blue complex, the intensity of which
456 depends on the amount of iodide remained in solution.
457
458
459
460
461
462
463
464
465

466 *2. 7. Mucoadhesion ex vivo assays*

467
468
469
470
471
472

473
474
475
476 *Ex vivo* experiments implied the collection of tissues from animals. All experiments that
477 involved the use of animals were performed following a protocol that was approved by the
478 ethic comity of the Ministry of Research and Superior Education in France (CEEA 26).
479

480 The mucoadhesive properties of the thiolated NPs were determined in Ussing-chambers
481 employing the surface of fresh intestinal tissue. Electrical parameters were also recorded to
482 determine the tissue viability and the opening of tight junctions during the assay.
483
484

485 The mucoadhesion experiments were carried out according to protocols previously described
486 [25]. Briefly, a jejunum portion isolated from fresh small intestine of sacrificed male Wistar
487 rats (200–250 g) (Charles River, Paris) was excised, rinsed with Ringer buffer and cut into
488 segments of 2–3 cm length. After visual examination of the tissue, sections of such jejunum
489 portion were mounted in Ussing chambers (the intestinal surface tested was 1 cm²), bathed
490 with Ringer solution at 7.4, the system was maintained at 37 °C and continuously oxygenated
491 with O₂/CO₂ (95%/5%). After 30 min of incubation, the liquid of the donor chamber was
492 replaced by the same volume (2 mL) of preheated (37 °C) Ringer solution containing the
493 fluorescence nanoparticle dispersion (5 mg/mL). At scheduled time intervals, four aliquots of
494 200 µL were withdrawn from the donor and from the acceptor chamber (mucosal and serosal
495 side, respectively) and replaced with the same volume of fresh medium pre-equilibrated at 37
496 °C. The tests were carried out for 120 min. At the end of the experiment (after 120 min), the
497 tissue was collected and degraded with 1 mL of a lytic solution (Sodium dodecyl sulfate, SDS
498 2 % v/v and NaOH 1 % v/v in MilliQ[®] water) for 24 h at 37 °C. The samples were analyzed
499 measuring the fluorescence of Rhodamine B with a spectrofluorimeter (L550B spectrometer,
500 Perkin Elmer, Norwalk, USA), emitting at 575 nm and excitation at 555 nm and using CS-
501 and GCS-P-NPs as controls. Four jejunum portions from four different rats were used to
502 evaluate each formulation and the experiments were replicated on different days. The
503 percentage of NPs stuck on 1 cm² of the mucosal surface (M%/cm²) was calculated using Eq.
504 (1)
505
506
507
508
509
510
511
512
513
514
515
516
517

$$518 \quad M\%/cm^2 = [F(m) - F(b)] / [F(t_0)] \times 100 \quad \text{Eq. (1)}$$

519 where F (m) was the fluorescence of the tissue treated with the dispersion of NPs, F (b) was
520 the fluorescence of the untreated intestinal tissue and F (t₀) was the fluorescence of the
521 nanoparticle dispersion before it was placed in contact with the intestinal tissue (at time 0).
522
523
524
525
526
527
528
529
530
531

The values of M % were calculated between 0 and 120 min after addition of the fluorescent NPs in all experiments.

2.7.1 Measurement of electrical parameters.

In the course of the mucoadhesion experiments, the transmucosal electrical resistance (TEER) was measured using a four electrode system according to the protocol previously described [25]. Briefly, transmucosal potential difference (PD) was continuously monitored between two KCl saturated agar bridges connected to an MDVC-2C voltage clamp (Titus Business Corporation, Paris, France) via calomel electrodes filled with saturated KCl solution. Potential difference was short-circuited throughout the experiment by a short-circuit current (Isc) via agar bridges placed in each half-cell, and adapted to platinum electrodes connected to an automatic MDVC-2C voltage clamp (Titus Business Corporation, Paris, France). Isc values were corrected for fluid resistance and recorded at scheduled times. The TEER was calculated from the Ohm's law (Eq. (2)):

$$\text{TEER} = \text{PD}/\text{Isc} \quad \text{Eq (2)}$$

Only tissues showing $\text{PD} > 2 \times 10^3 \text{V}$ and $\text{Isc} > 40 \times 10^{-6} \text{A}/\text{cm}^2$ after 30 min incubation were included in the study. At the end of the experiment, a further control was performed by adding 90 μL of a 10^{-3}M histamine Ringer buffer solution in the serosal compartment. Histamine increases Cl^- secretion by the cells with consequent enhancement of Isc. Whenever no increase in Isc was observed, damages in the tissue were suspected and all samples collected from the corresponding chambers were discarded.

2. 7.2. Quantification of attached nanoparticles to intestinal mucosa

The number of attached NPs to intestinal mucosa (N) was calculated from Eq (3):

$$N = M_T / \rho \pi d^3 \quad \text{Eq (3)}$$

where M_T is the mass of both attached and non-attached NPs (g) incubated with intestinal mucosa, ρ is the NPs volumetric mass ($1.2 \text{g}/\text{cm}^3$ (24)), d is the NP hydrodynamic diameter (cm). M_T , in turn, was calculated taking into account the volume of the donor compartment of the Ussing-chamber (2 mL) and the nanoparticle dispersion concentration (5 mg/mL). By the percentage of NPs stuck on 1cm^2 of the mucosal surface (*i.e.*, $\text{M}\%/\text{cm}^2$, Eq. (1)) it was possible to calculate the number of attached NPs to the intestinal mucosa.

On the other hand, the number of theoretical layers of nanoparticles covering an apparent surface area of intestinal mucosa of 1 cm² may be calculate as suggested by Bravo-Osuna *et al* [24] using the following Eq (4):

$$\text{Number of theoretical layers} = Nd^2 \quad \text{Eq (4)}$$

2. 8 Statistical analysis

Statistical comparisons were performed utilizing analysis of variance (ANOVA) followed by the Tukey post hoc tests (GraphPad Prism v. 4 for Windows, Graph-Pad Software, San Diego, CS). Differences were considered statistically significant at $p < 0.05$.

3. Results and Discussion

The aim of the present study was to compare the mucoadhesive properties of PIBCA NPs coated with LMW-CS and -CS thiomers with those of the corresponding PIBCA NPs coated with LMW-GCS and -GCS thiomers. Among the thiolate polymers currently known, our attention was focused on those modified with *N*-acetyl cysteine (NAC) and reduced glutathione (GSH). In addition to their interesting mucoadhesive properties, these thiomers are endowed with interesting permeation-enhancing and P-gp inhibitory characteristics [10,18]. For the mentioned purpose, the required NPs were prepared following the radical polymerization method described by Chauvierre *et al* [27-29]. Table 1 summarizes the hydrodynamic mean diameters of all the nanoparticles synthesized for this study. The mean hydrodynamic diameter of CS- and thiolated CS- coated NPs was about twice that observed for GCS-based NPs.

[Insert Table 1]

This result can be accounted for the average molecular weight of the starting unmodified CS. Depolymerization of GCS with HNO₂, indeed, leads to a significant reduction of molecular weight up to 7 kDa at pH ≤ 3 (26) which is quite lower than that of the CS used in this study (*i.e.*, 20 kDa). Consistently with data of the literature, the size of PIBCA NPs generated by radical emulsion polymerization synthesized in this work depended on the molecular weight of the polysaccharide [24, 28]. Moreover, the size of thiolated CS- and thiolated GCS-coated NPs (*i.e.*, CSGSH-P-NP, GCSGSH-P-NP) was increased by half of the size of the corresponding non thiolated nanoparticles (CS-P-NP, GCS-P-NP, respectively). Rhodamine B loaded NPs showed almost the same size of unloaded and the differences were not

650
651
652 significant (data not shown). Consistently with the polycationic nature of the material used to
653 coat the nanoparticles, zeta potential of all nanoparticles were positive. The value depended
654 on the type of polysaccharide and on the pH value of the nanoparticle dispersion. The highest
655 values of zeta potential found in acidic pH agreed with a protonation of the polysaccharide at
656 this pH. The PDI values observed for CS-P-NPs and GCS-P-NPs (*i.e.*, 0.05 and 0.04,
657 respectively), are indicative of a quite homogeneous dispersion in size of these NPs, while a
658 much more large size dispersion was observed for the other NPs since their PDI values were
659 in the range 0.26-0.58. Thus, the PDI values clearly showed that NPs coated with thiomers
660 were more hetero-dispersed than the corresponding unmodified parent polymer-coated NPs
661 and this may be explained by a higher average molecular weight of the thiomers used.

662
663 The morphology of the NPs was studied by TEM. Electron micrographs indicated that the
664 NPs are generally spherical in shape (Figure 2).

665
666 [Insert Figure 2]

667
668 The amount of free thiol groups on the surface of thioimer-coated PIBCA NPs was
669 determined by iodometric titration using a calibration curve ($y = -0.0311x + 0.1004$ $R^2 =$
670 0.981) obtained with different concentrations of cysteine-HCl, and the results are also showed
671 in Table 1. As can be seen, it was found that the amount of free thiol groups on the surface of
672 GCS thioimer-coated PIBCA NPs was lower than the corresponding NPs coated with CS
673 thiomers.

674
675 The mucoadhesive performances of the studied NPs were evaluated on mucosa of fresh
676 intestinal tissue after 2 h of contact in Ussing-chambers. The *in vitro* mucoadhesive studies
677 employing the Ussing-chamber technique are significant enough for evaluating the
678 mucoadhesive potential of NPs and offer many advantages, including more bio-mimetic
679 conditions, over other *in vitro* mucoadhesive tests. A distinct advantage of the Ussing
680 chambers is that they allow the monitoring of the trans-epithelial electrical potential (TEER)
681 of the intestinal tissues during the experiment [31]. Variation of TEER overtime indicates the
682 opening of tight junctions while the viability and integrity of the mucosa was controlled. In
683 general, control of the integrity of the tissue consists on addition of pump inhibitors at the end
684 of the experiments inducing so a voluntary variation of TEER due to the increased
685 permeability of the tissue by paracellular routes. Having controlled the integrity of the tissue
686 at the end of the experiment, a variation of TEER observed in the present work could indicate
687 that the formulation increased the permeability of the mucosa. Results obtained from
688 mucoadhesive studies are shown in Table 2. In general, thioimer-coated NPs adhered in a
689
690
691
692
693
694
695
696
697
698
699
700
701
702
703
704
705
706
707
708

709
710
711
712 higher extend on the mucosal surface than the corresponding NPs coated with the non-
713 thiolated parent polysaccharide. The GCSNAC-P-NPs seemed to display a different
714 mucoadhesion compared with that monitored with GCS-P-NPs, the ANOVA demonstrated
715 that there was no significant difference of interaction with the mucus between these GCS-
716 based nanocarriers.
717
718
719

720
721 [Insert Table 2]
722

723 Despite the low surface thiol group content and the moderate positive zeta potential (*i.e.*, +31
724 ± 1 mV), GCSGSH-P-NPs exhibited the highest mucoadhesivity as demonstrated by the high
725 percentage of NPs attached on the rat intestinal surface (*i.e.*, 76.3 %/cm²). The results that are
726 generally consistent with those of the literature were obtained in very different experimental
727 conditions [25,30]. Indeed, here, mucoadhesion studies were performed in Ussing chambers
728 in which the mucosa was placed in vertical position while it was surrounded by significant
729 volumes of survival medium on both side of the mucosae. The nanoparticles added in the
730 donor compartment were rather diluted and maintained under agitation while the design of
731 the experimental conditions were designed to maintain the viability and functionality of the
732 tissue. In contrast, in previous works evaluating mucoadhesion of chitosan/thiolated chitosan-
733 coated PIBCA NPs, a small volume of the dispersion of nanoparticles was placed directly on
734 the luminal side of the intestinal tissue mounted on the horizontal position in a device that
735 only allowed to expose a well define surface area of the tissue to samples to be tested. In this
736 model, no condition was provided to maintain the viability and functionality of the tissue.
737 The mucoadhesion of the nanoparticles considered in the present work was evaluated from
738 the calculation of the number of NPs attached to mucosa. Results were reported in Table 2.
739 Besides, calculations were performed to estimate the number of theoretical NPs layers
740 formed onto the 1 cm² mucosal apparent surface area. These calculations suggested that the
741 nanoparticles adhered on the mucosa forming several layers. However, it is noteworthy that
742 the apparent surface area that was taken in the calculation can underestimated the actual
743 surface area available on the mucosa surface. Indeed, in the apparent surface area calculated
744 from the geometry of the aperture separating the two compartments of the Ussing chamber
745 the roughness of the mucosal surface created by villi were not taken into account.
746 Nevertheless, this result indicated that a huge amount of nanoparticles adhered on the mucosa
747 eventually covering the mucosa surface by the accumulation of several layers of
748 nanoparticles. The nanoparticles that adhered the most were GCSGSH-P-NPs. Consistently
749
750
751
752
753
754
755
756
757
758
759
760
761
762
763
764
765
766
767

768
769
770 with data of the literature, the hydrodynamic diameter of the nanoparticles seemed to play an
771 important role influencing the transport by diffusion phenomena through the mucus layer and
772 hence the mucoadhesion properties of CS coated PIBCA NPs [24,32]. In Figure 3a, the
773 amount of attached NPs has been plotted against the hydrodynamic mean diameter observed
774 by QELS. Besides the superior mucoadhesive properties of GCSGSH-P-NPs, in the
775 remaining cases, a negative correlation between the number of attached NPs and their
776 hydrodynamic mean diameter was noted consistently with results already reported on
777 thiolated chitosan-coated PIBCA nanoparticles [24,32]. In Figure 3b, the number of attached
778 NPs was plotted against the content free thiol groups at the NPs surface. As shown, a
779 negative exponential correlation between the number of attached NPs and their free thiol
780 content was observed. Again, the highest number of NPs attached was noted for GCSGSH-P-
781 NPs despite their low surface thiol group amount. These findings are also in agreement with
782 data obtained by Bravo-Osuna *et al* [24] in the same range of the surface thiol group amount
783 and at the same NPs concentration. As observed by these authors, in fact, a decrease in
784 mucoadhesion occurred when the surface thiol group content was lower than 0.02 μmol
785 SH/cm^2 . Finally, since it was also suggested that enhanced electrostatic interactions take
786 place between CS-coated PIBCA NPs and glycoproteins of mucus [24], it was of interest to
787 examine the effect of ζ potential as function of the free thiol content at the NPs surface.
788 However, as shown in Figure 3c, no clear correlation could be observed between the number
789 of attached NPs and their surface charge, again according to that previously reported with
790 CS-coated PIBCA NPs and evaluated by another method [24].
791
792
793
794
795
796
797
798
799
800
801
802
803
804

805 [Insert Figure 3]

806 Taken together, all these results indicated that, in the series herein examined, the highest
807 mucoadhesion properties was observed with a hydrodynamic diameter of about 300 nm
808 corresponding to the size of the GCSGSH-P-NPs. This finding agreed well with the results of
809 previous studies suggesting that hydrodynamic diameters in the range 200-300 nm may be
810 considered optimal for a satisfactory interaction with mucus chains [24,32]. Consequently, it
811 may account for the lower mucoadhesive properties of CS-P-, CSNAC-P- and CSGSH-P-NPs
812 characterized by larger hydrodynamic diameters (*i.e.*, 400-600 nm). In this context, however,
813 it was surprising that the mucoadhesion of GCSNAC-P-NPs appeared much lower than that
814 of GCSGSH-P-NPs despite the former nanocarriers were endowed with a size of 296 nm, a
815 high zeta potential ($+49 \pm 1\text{mV}$) and a higher concentration of thiol groups on the surface.
816 Even though this aspect remains to be fully clarified, to explain the marked difference in
817
818
819
820
821
822
823
824
825
826

827
828
829
830 mucoadhesive properties between GCSNAC-P-NPs and GCSGSH-P-NPs, additional
831 parameters should be considered including flexibility of the macromolecules, electrostatic
832 interactions, molecular weight of the polymer chains as well as swelling, ionic strength and
833 pH of the medium. In fact, according to the accepted mechanism for the mucoadhesion
834 process [33], two sequential steps should be considered and namely, a first contact stage
835 where a close contact between mucoadhesive polymer and mucus occurs. In the second one,
836 *i.e.*, the so-called “consolidation stage”, several physical (noncovalent) and chemical
837 (covalent) interactions are established between the mucoadhesive polymer and mucus
838 glycoproteins. In this consolidation stage, a chain interpenetration and entanglement takes
839 place leading to strong enough adhesion. The chain flexibility, which is directly related to
840 chemical structure and molecular weight of the polymer, is thought to be important in the
841 consolidation stage since it allows the approach of binding groups and consequent
842 interpenetration and entanglement of macromolecules. Thus, it can be hypothesized that
843 introduction of GSH moieties on the GCS polymeric backbone constituting the shell of the
844 corresponding PIBCA NPs leads to more flexible chains than those resulting from covalently
845 linking NAC to GCS [16]. A further aspect to be taken into account refers to the fact that,
846 introduction of GSH moieties, but not the NAC ones, on the GCS polymeric backbone can
847 positively influence the water solubility of the coating polymer GCSGSH leading to its
848 swelling with consequent improved flexibility and, hence, enhanced mucoadhesive
849 properties.

850
851
852 Moreover, it should be also considered that, unlike GCSNAC, GSH moieties linked to GCS
853 polymer contain ionizable carboxyl groups. Considering the pH of the buffer employed in the
854 Ussing chamber experiments (*i.e.*, 7.4), these groups should be in dissociate form. Thus, they
855 may be involved in electrostatic and non-covalent interactions with mucus components hence
856 enhancing the mucoadhesion of the GCSGSH-P-NPs.

857
858 Besides the percentage of NPs stuck on the mucosal surface after 2 h of contact, it was also
859 measured by fluorescence intensity both in the donor and in the acceptor compartment of the
860 Ussing chamber in the presence of NPs. As shown in Figure 4, the fluorescence intensity was
861 markedly reduced after 120 min in the donor compartment, while, in the acceptor
862 compartment, the fluorescence was negligible (data not shown). This suggests that these NPs
863 were stuck on the mucosal surface remaining firmly adherent to the surface of the intestinal
864 lumen without crossing of the intestinal tissue

880 [Insert Figure 4]

886
887
888
889 The incubation of the different nanoparticle formulations with the intestinal tissue induced
890 changes in TEER. In contrast to that observed with the CS- and thiolated CSs, when thiolated
891 GCS-based coatings were used, the TEER was lower than that measured with the unmodified
892 polymer after 120 min of incubation time. Figure 5 shows the TEER % changes induced by
893 the different NPs formulations between 30 min and 120 min incubation time. The notable
894 decrease of TEER values with GCSNAC-P-NPs and CSGSH-P-NPs between 60-120 min of
895 incubation time, suggests an enhancement of the paracellular transport when these colloidal
896 GCS-based carriers were employed. Hence, they can bring about a permeation effect since
897 they induce an enlargement of epithelial cell tight junctions but the nanoparticles remained
898 unable to go across the epithelium. Nevertheless, the increase of permeability of the tight
899 junctions may be interesting to promote the absorption of poorly absorbed drug molecules
900 that could then be absorbed through this route. It is in agreement with results reported by
901 other authors who observed by Ussing-type techniques a permeation of thiolated CS higher
902 than that observed for the unmodified polymer [34].
903
904
905
906
907
908
909
910

911 [Insert Figure 5]

912 A model can be proposed to explain the mucoadhesion of the nanoparticles developed in the
913 present work and their permeation enhancing properties (Figure 6). In a first step, the
914 nanoparticles penetrate in the hydrogel mucus thanks to convection and Brownian motions.
915 Then, they are retained in the mucus due to the occurrence of electrostatic interactions and
916 formation of di-sulfur bonds between the polymer chains of the nanoparticle shell and
917 complementary groups found on mucin glycoproteins (Figure 6a). The particle size notably
918 influence the penetration and diffusion step and we believe that the differences observed
919 between the GCS/GCS thiomers-based NPs and the corresponding CS/CS thiomers ones were
920 mainly due to differences in their respective hydrodynamic diameters. Finally, nanoparticles
921 interacting the most with the mucosa, the CSGSH-P- and GCSNAC-P-core-shell NPs, were
922 able to increase the permeability of the paracellular route that involved the opening of
923 epithelial cell tight junctions (figure 6b). This was possible assuming that the nanoparticles
924 could deeply penetrate in the mucus layer thanks to their smaller size and could interact with
925 proteins of the tight junctions of the underlying epithelium thanks to their thiol groups. The
926 last type of interactions can induce conformational changes of the tight junction proteins
927 leading to leakage of the tight junctions increasing the permeability of the epithelium through
928 the paracellular route [16,17,34].
929
930
931
932
933
934
935
936
937
938
939

940 [Insert Figure 6]

Conclusions

Novel PIBCA NPs coated with thiol derivatives of LMW-CS, -GCS and corresponding unmodified parent polymers were successfully prepared and characterized. All these new colloidal systems showed mucoadhesive properties as evaluated by the Ussing-chamber technique. In this way, it was found that GCSGSH-P-NPs possessed the most favorable mucoadhesive performances. Data also showed that the mucoadhesive properties of all the polymers examined can be arranged in the following rank order: GCSGSH-P- >> GCS-P- ~ GCSNAC-P- > CS-P- > CSNAC-P- ~ CSGSH-P-NPs. These results were interpreted on the basis of literature suggestions concerning both the mucoadhesion process of CS- and thiolated CS-PIBCA core shell NPs and the basic principles underlying the mechanism of mucoadhesion. Moreover, both GCSGSH-P- and GCSNAC-P-core-shell NPs showed an enhancement of the paracellular transport without crossing of the intestinal tissue. This effect may be an advantage from a toxicological point of view and it is probably due to the capability of the latter NPs to only enlarge the epithelial cell tight junctions as proved by TEER measurements. Therefore, LMW- GCSGSH-P- and GCSNAC-P-NPs may be considered new and interesting delivery systems for enhanced absorption of different kind of drugs including peptides, proteins and anticancer drugs by transmucosal administration, thanks to their mucoadhesion and permeation promoter effect on tight junctions.

Acknowledgments

This work is part of the PhD thesis of CP. This work was supported by grants from MIUR (Ministero dell'Istruzione, dell'Università e della Ricerca), Progetto PRIN 2010–2011 2010H834LS_005 to A.T., G.T. The present work has benefited from the facilities and expertise of the Electron Microscopy facilities of I2BC, CNRS, Gif sur Yvette, France (<http://www.cgm.cnrs-gif.fr/spip.php?article282&lang=fr>).

References

1. S. Barbault-Foucher, R. Gref., P. Russo, J. Guechot, A. Bochot, Design of poly-epsilon-caprolactone nanospheres coated with bioadhesive hyaluronic acid for ocular delivery. *J. Control. Release* 83(3) (2002) 365-75.
2. G. Ponchel, J. Irache, Specific and non-specific bioadhesive particulate systems for oral delivery to the gastrointestinal tract. *Adv. Drug Deliv. Rev.* 34(2-3) (1998) 191-219.

- 1004
1005
1006
1007 3. Y. Huang, W. Leobandung, A. Foss, N. A. Peppas, Molecular aspects of muco- and
1008 bioadhesion: tethered structures and site-specific surfaces. *J. Control. Release* 65(1-2) (2000)
1009 63-71.
1010
1011
1012 4. D. Dodou, P. Breedveld, P.A. Wieringa, Mucoadhesives in the gastrointestinal tract:
1013 revisiting the literature for novel applications. *Eur. J Pharm. Biopharm.* 60(1) (2005) 1-16.
1014
1015
1016 5. M. C. Rose, J. A. Voynow, Respiratory tract mucin genes and mucin glycoproteins in
1017 health and disease. *Physiol. Rev.* 86(1) (2006) 245-278.
1018
1019
1020 6. C.-M. Lehr, J. A. Bouwstra, H. E. Boddé, H. E. Junginger, A surface energy analysis of
1021 mucoadhesion: contact angle measurements on polycarbophil and pig intestinal mucosa in
1022 physiologically relevant fluids. *Pharm. Res.* 9(1) (1992) 70-75.
1023
1024
1025 7. M. Dasha, F. Chiellini, R. M. Ottenbrite, E. Chiellini, Chitosan-A versatile semi-synthetic
1026 polymer in biomedical applications. *Prog. Polym. Sci.* 36 (2011) 981–1014.
1027
1028
1029 8. A. Trapani, J. Sitterberg, U. Bakowsky, T. Kissel, The potential of glycol chitosan NPs as
1030 carrier for low water soluble drugs. *Int. J. Pharm.* 375 (2009) 97–106.
1031
1032
1033 9. A Trapani, S. Di Gioia, N. Ditaranto, N. Cioffi, F.M. Goycoolea, A. Carbone, M. Marcos
1034 Garcia-Fuentes, M. Conese, M. J. Alonso, Systemic heparin delivery by the pulmonary route
1035 using chitosan and glycol chitosan NPs. *Int. J. Pharm.* 447 (1-2) (2013) 115-123.
1036
1037
1038 10. A. Trapani, C. Palazzo, M. Contino, M.G. Perrone, N. Cioffi, N. Ditaranto, N.A.
1039 Colabufo, M. Conese, G. Trapani, G. Puglisi, Mucoadhesive properties and interaction with
1040 P-glycoprotein (P-gp) of thiolated-chitosans and -glycol chitosans and corresponding parent
1041 polymers: a comparative study. *Biomacromolecules* 15(3) (2014) 882-93.
1042
1043
1044 11. S. Mao, X. Shuai, F. Unger, M. Simona, D. Bi, T. Kissel. The depolymerization of
1045 chitosan: effects on physicochemical and biological properties. *Int. J. Pharm.* 281 (2004) 45–
1046 54.
1047
1048
1049 12. C.E. Kast, W. Frick, U. Losert, A. Bernkop-Schnurch, Chitosan-thioglycolic acid
1050 conjugate: a new scaffold material for tissue engineering? *Int. J. Pharm.* 256(1-2) (2003).
1051 183-189.
1052
1053
1054
1055
1056
1057
1058
1059
1060
1061
1062

- 1063
1064
1065
1066 13. A. Bernkop-Schnurch, M. Hornof, T. Zoidl, Thiolated polymers--thiomers: synthesis and
1067 in vitro evaluation of chitosan-2-iminothiolane conjugates. *Int. J. Pharm.* 260(2) (2003); 229-
1068 237.
1069
1070
1071 14. K. Kafedjiiski, M. Hoffer, M. Werle, A. Bernkop-Schnurch, Improved synthesis and in
1072 vitro characterization of chitosan-thioethylamidine conjugate. *Biomaterials* 27(1) (2006) 127-
1073 135.
1074
1075
1076
1077 15. T. Schmitz, V. Grabovac, T. F. Palmberger, M. H. Hoffer, A. Bernkop-Schnurch,
1078 Synthesis and characterization of a chitosan-*N*-acetyl cysteine conjugate. *Int. J. Pharm.*
1079 347(1-2) (2008) 79-85.
1080
1081
1082
1083 16. K. Kafedjiiski, F. Foger, M. Werle, A. Bernkop-Schnurch, Synthesis and in vitro
1084 evaluation of a novel chitosan-glutathione conjugate. *Pharm. Res.* 22(9) (2005) 1480-1488.
1085
1086
1087 17. V.M. Leitner, G.F. Walker, A. Bernkop-Schnurch, Thiolated polymers: evidence for the
1088 formation of disulphide bonds with mucus glycoproteins. *Eur. J. Pharm. Biopharm.* 56(2)
1089 (2003) 207-214.
1090
1091
1092 18. T. Schmitz, J. Hombach, A Bernkop-Schnürch, Chitosan-*N*-acetyl cysteine conjugates: In
1093 vitro evaluation of permeation enhancing and P-glycoprotein inhibiting properties. *Drug*
1094 *Delivery* 15 (2008) 245–252.
1095
1096
1097
1098 19. S. Mazzaferro, K. Bouchemal, G. Ponchel, Oral delivery of anticancer III: formulation
1099 using drug delivery systems. *Drug Discov. Today* 18 (2013) 99-104.
1100
1101
1102 20. C. Damge', C. Michel, M. Aprahamian, P. Couvreur, New approach for oral
1103 administration of insulin with poly-alkylcyanoacrylate nanocapsules as drug carrier. *Diabetes*
1104 37 (1988) 246–251.
1105
1106
1107
1108 21. J.L. Grangier, M. Puygrenier, J.C. Gautier, P. Couvreur, Nanoparticles as carriers for
1109 growth hormone releasing factor. *J. Control. Release* 15(1) (1991) 3–13.
1110
1111
1112 22. M.B.F. Martins, S.I.D. Simoes, A. Supico, M.E.M. Cruz, R. Gaspar, Enzyme-loaded
1113 PIBCA NPs (SOD and L-ASNase): optimization and characterization. *Int. J. Pharm.* 142(1)
1114 (1996) 75–84.
1115
1116
1117
1118
1119
1120
1121

- 1122
1123
1124
1125 23. G. Lambert, E. Fattal, A. Brehier, J. Feger, P. Couvreur, Effect of
1126 polyisobutylcyanoacrylate NPs and Lipofectins loaded with oligonucleotides on cell viability
1127 and PKCa neosynthesis in HepG2 cells. *Biochimie* 80(12) (1998) 969–976.
1128
1129
1130 24. I. Bravo-Osuna, C. Vauthier, A. Farabollini, G. F. Palmieri, G. Ponchel, Mucoadhesion
1131 mechanism of chitosan and thiolated chitosan-poly(isobutyl cyanoacrylate) core-shell NPs.
1132 *Biomaterials* 28(13) (2007) 2233-2243.
1133
1134
1135 25. I. Bravo-Osuna, C. Vauthier, H. Chacun, G. Ponchel, Specific permeability modulation of
1136 intestinal paracellular pathway by chitosan-poly(isobutylcyanoacrylate) core-shell
1137 nanoparticles. *Eur. J. Pharm. Biopharm.* 69(2) (2008) 436-444.
1138
1139
1140 26. D.K. Knight, S.N. Shapka, B.G. Amsden, Structure, depolymerization, and
1141 cytocompatibility evaluation of glycol chitosan. *J. Biomed. Mater. Res. A*, 83(3) (2007) 787-
1142 798.
1143
1144
1145 27. C. Chauvierre, D. Labarre, P. Couvreur, C. Vauthier, Radical polymerization of
1146 alkylcyanoacrylates initiated by the redox system dextran-cerium (IV) under acidic aqueous
1147 conditions. *Macromol.* 36 (2003) 6018–6027.
1148
1149
1150 28. C. Chauvierre, D. Labarre, P. Couvreur, C. Vauthier, Plug-in spectrometry with optical
1151 fibres as a novel analytical tool for NPs technology: application to the investigation of the
1152 emulsion polymerisation of the alkylcyanoacrylate. *J. Nano Res.* 5 (2003) 365–371.
1153
1154
1155 29. C. Chauvierre, D. Labarre, P. Couvreur, C. Vauthier, Novel polysaccharide-decorated
1156 poly(isobutyl cianoacrylate) nanoparticles. *Pharm. Res.* 20(11) (2003) 1786–1793.
1157
1158
1159 30. I. Bravo-Osuna, D. Teutonico, S. Arpicco, C. Vauthier, G. Ponchel, Characterization of
1160 chitosan thiolation and application to thiol quantification onto nanoparticle surface. *Int. J.*
1161 *Pharm.* 340(1-2) (2007) 173-181.
1162
1163
1164 31. P. Mardones, D. Andrinolo, A. Csendes, N. Lagos, Permeability of human jejunal
1165 segments to gonyautoxins measured by the Ussing chamber technique. *Toxicol.* 44(5) (2004)
1166 521-528.
1167
1168
1169
1170
1171
1172
1173
1174
1175
1176
1177
1178
1179
1180

1181
1182
1183
1184 32. I. Bravo-Osuna, T. Schmitz, A. Bernkop-Schnürch, C. Vauthier, G. Ponchel, Elaboration
1185 and characterization of thiolated chitosan-coated acrylic nanoparticles. *Int. J. Pharm.* 316
1186 (2006) 170-175.
1187

1188
1189 33. J.D. Smart, The basics and underlying mechanisms of mucoadhesion. *Adv. Drug Deliv.*
1190 *Rev.* 57 (2005) 1556–1568.
1191

1192
1193 34. F. Foger, T. Schmitz, A. Bernkop-Schnürch, In vitro evaluation of an oral delivery system
1194 for P-gp substrates based on thiolated chitosan. *Biomaterials* 27 (2006) 4250-4255.
1195
1196
1197
1198
1199
1200
1201
1202
1203
1204
1205
1206
1207
1208
1209
1210
1211
1212
1213
1214
1215
1216
1217
1218
1219
1220
1221
1222
1223
1224
1225
1226
1227
1228
1229
1230
1231
1232
1233
1234
1235
1236
1237
1238
1239

Captions to Figures

Figure 1. Schematic representation of the low molecular weight chitosan- or glycolchitosan- and corresponding thiomers-coated poly(isobutylcyanoacrylate) core-shell nanoparticles prepared in this study.

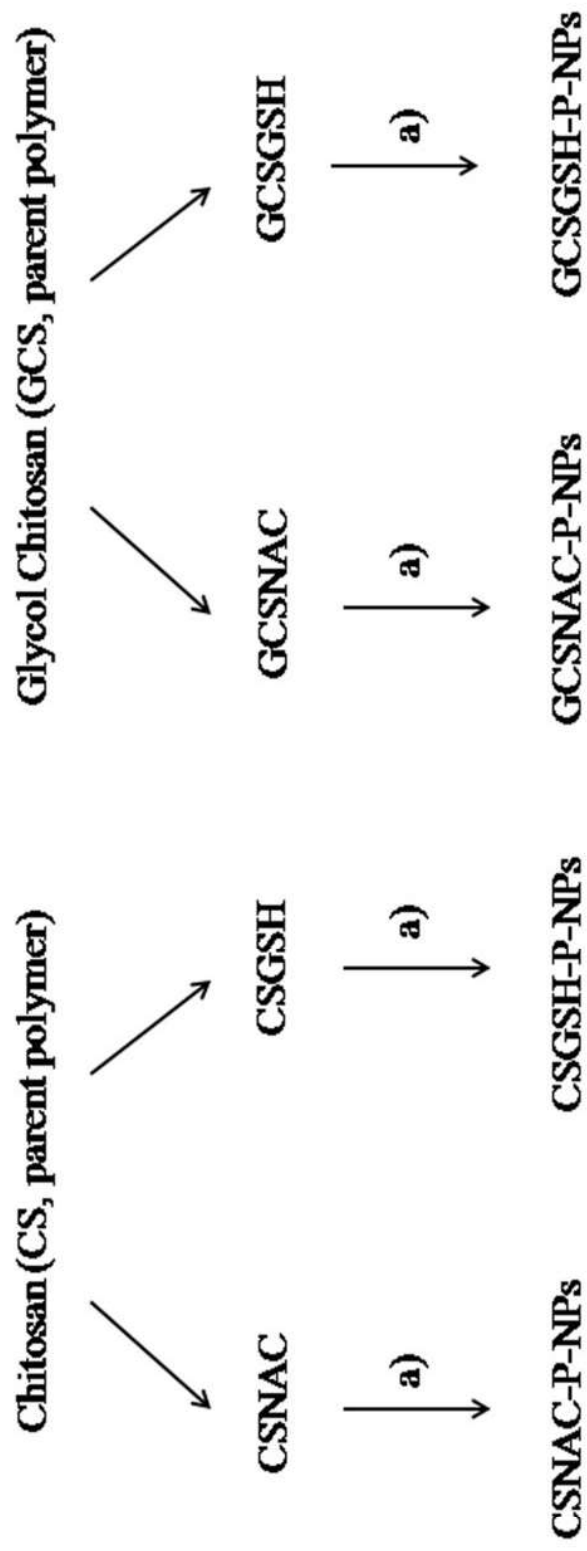
Figure 2. Transmission electron microscopy images of CS-P-NPs a), CSNAC-P-NPs b), CSGSH-P-NPs c), GCS-P-NPs d), GCSNAC-P-NPs e) GCSGSH-P-NPs f).

Figure 3. Effect of various parameters on the number of attached nanoparticles (5 mg/mL concentration) on intestinal mucosa in Ussing chambers. See Figure 2 for legend. a: nanoparticle hydrodynamic diameter b: free thiol content, c: nanoparticle ζ potential.

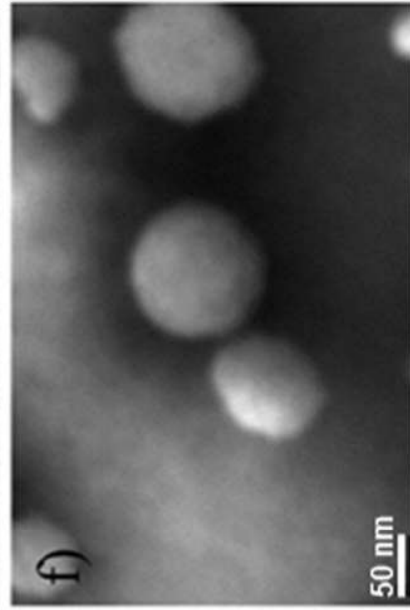
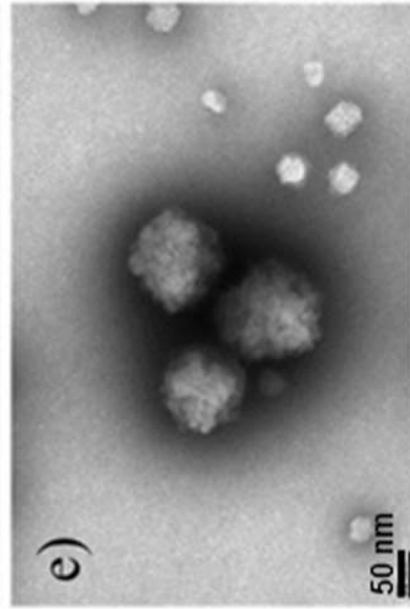
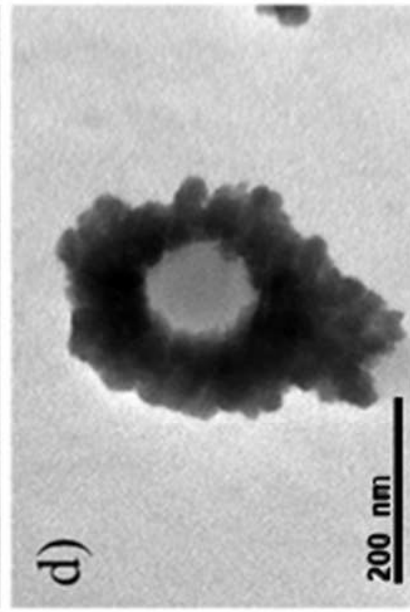
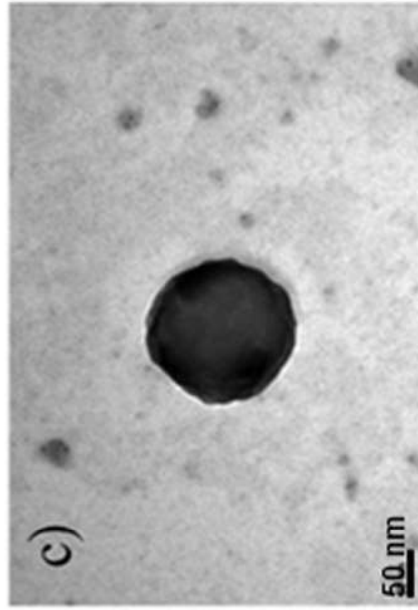
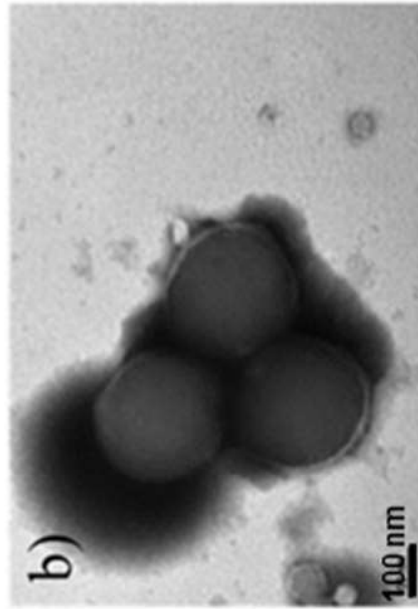
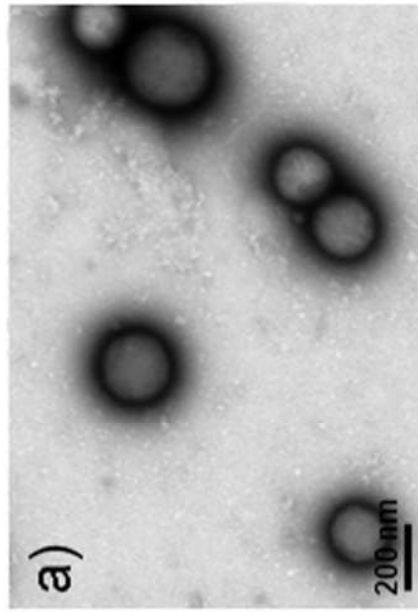
Figure 4. Variation in fluorescence in Ussing donor chamber in the presence of CSNAC-P-NPs, CSGSH-P-NPs, CS-P-NPs, GCSNAC-P-NPs, GCSGSH-P-NPs and GCS-P-NPs.

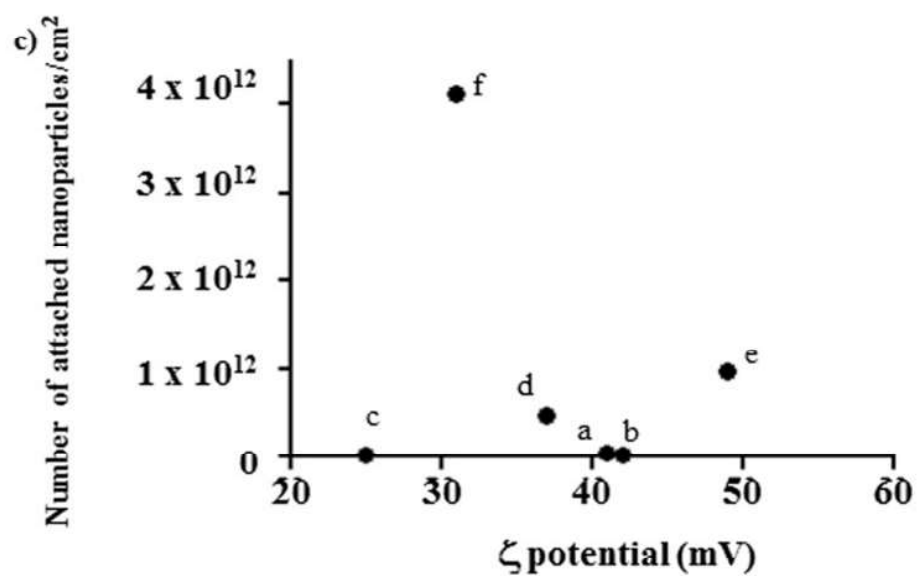
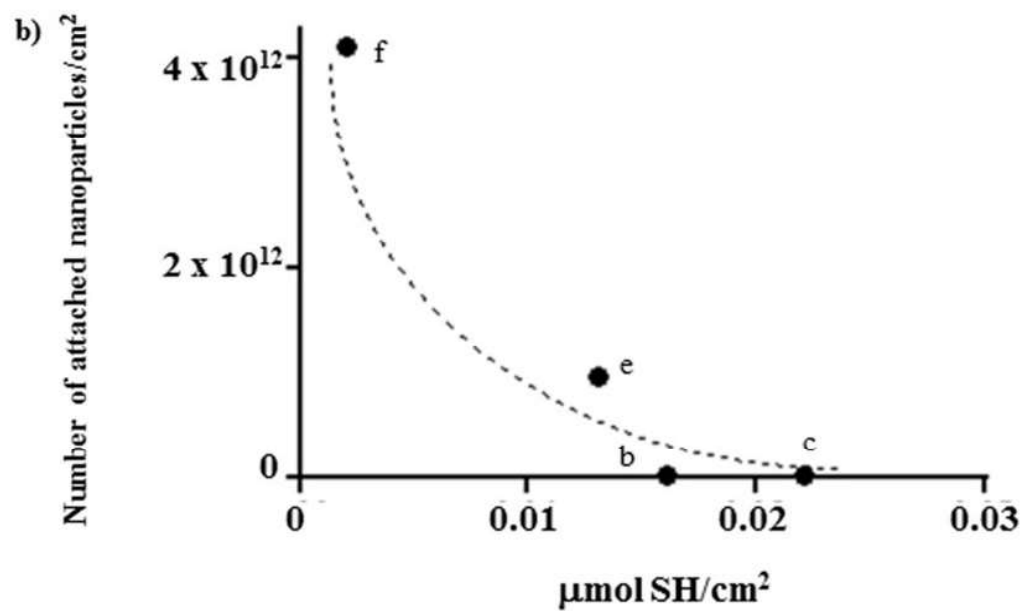
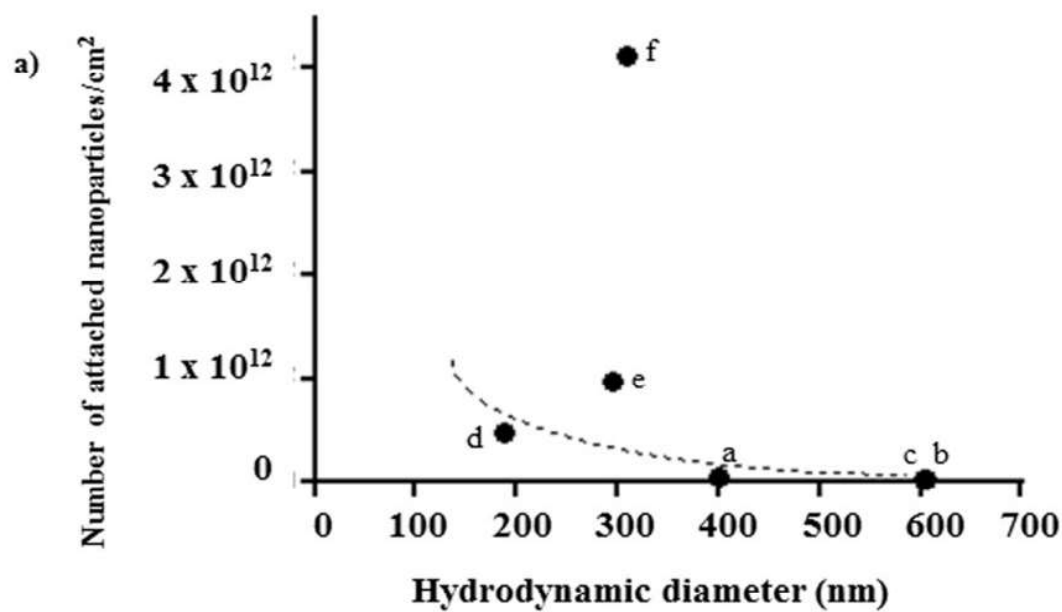
Figure 5. TEER % changes induced by the different NPs formulations between 30 min and 120 min incubation time.

Figure 6. Schematic representation of the interaction of nanoparticles with the mucin glycoproteins in the *attachment* step of the mucoadhesion process (a) and interactions with the underlying epithelium (b).

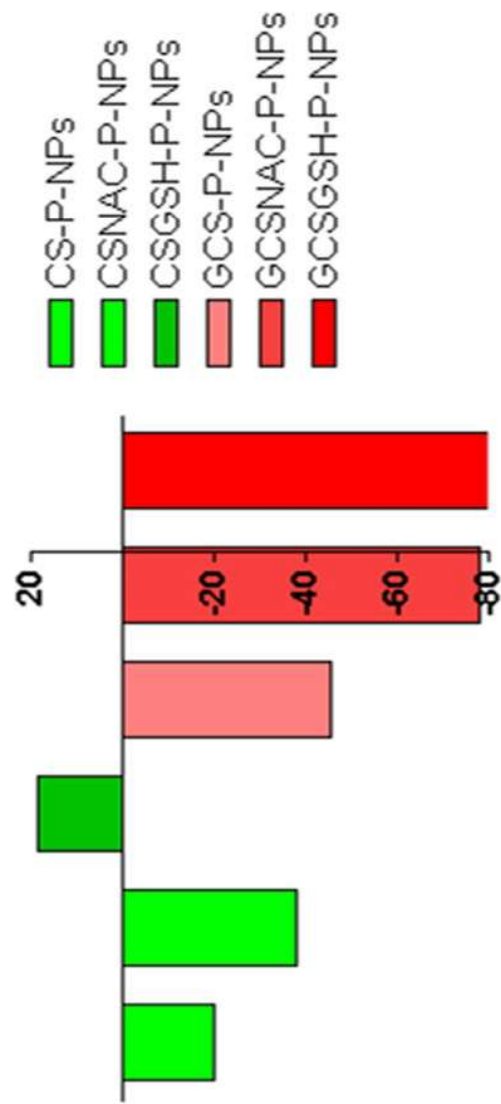


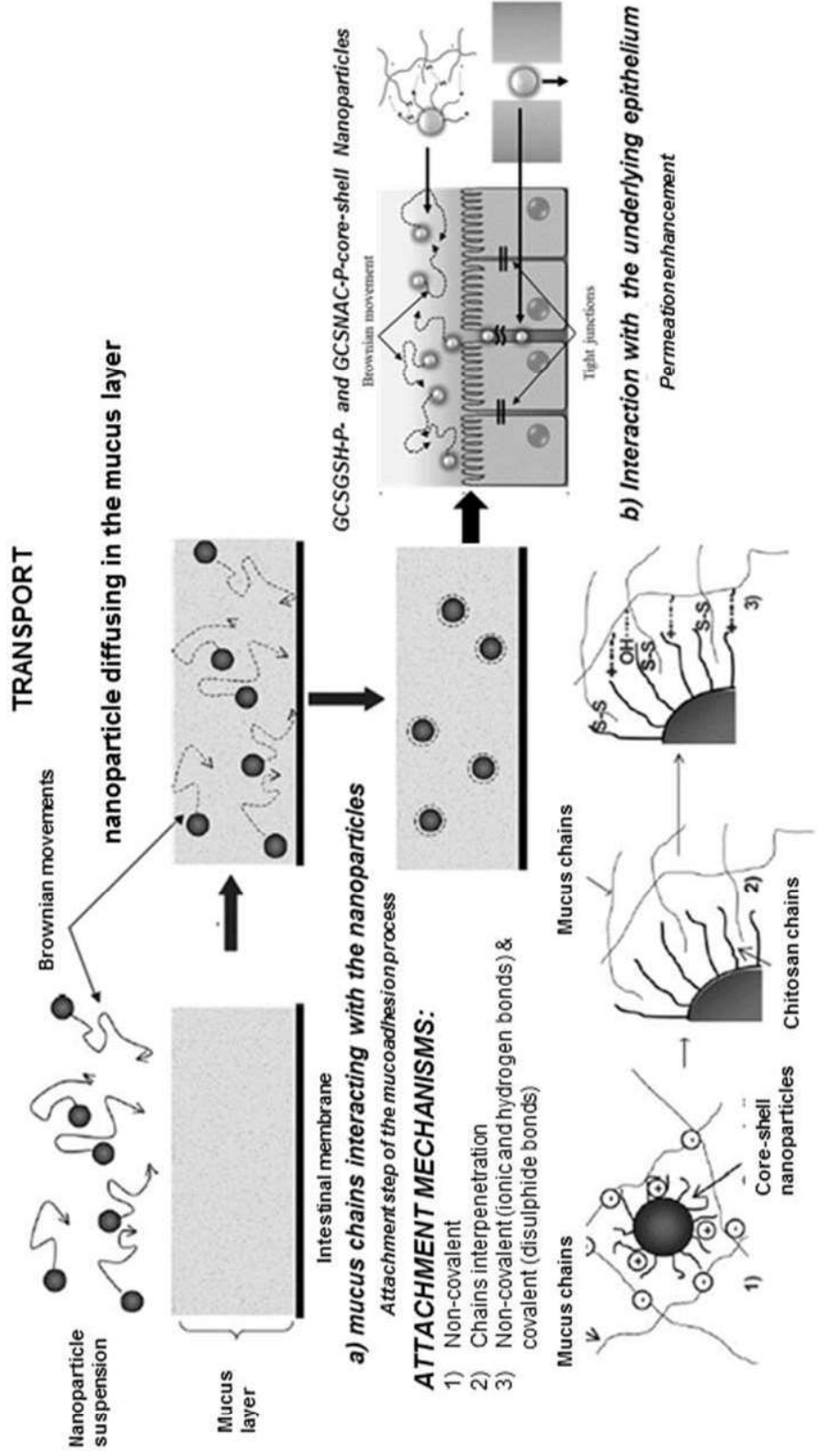
a) PIBCA (P)-NPs





THIR changes induced by the different NPs formulations (%)





Tab 1. Size, polydispersity index (PDI) and zeta potential (Z), and surface thiol content of LMW CS⁻, GCS- and corresponding thiomers-coated polyisobutyrylcyanoacrylate NPs.

	CS-P-NPs^a	CSNAC-P-NPs^a	CSGSH-P-NPs^a	GCS-P-NPs^b	GCSNAC-P-NPs^b	GCSGSH-P-NPs^b
Size (nm)	400 ± 9	605 ± 15	603 ± 98	187 ± 2	296 ± 19	309 ± 11
PDI	0.05 ± 0.00	0.26 ± 0.10	0.58 ± 0.20	0.04 ± 0.00	0.32 ± 0.10	0.33 ± 0.00
ζ at pH 2.5 (mV)	+ 41 ± 1	+ 42 ± 2	+ 25 ± 1	+ 37 ± 1	+ 49 ± 1	+ 31 ± 1
ζ at pH 7.0 (mV)	+ 23 ± 1	+ 9 ± 0	+ 2 ± 0	+ 16 ± 0	+ 2 ± 0	- 6 ± 1
μmol SH/cm²		160 x 10 ⁻⁴	220 x 10 ⁻⁴		130 x 10 ⁻⁴	20 x 10 ⁻⁴

^a Nanoparticles prepared from CS 20 kDa. ^b Nanoparticles prepared from GCS 7 kDa.

Table 2. Percentage of nanoparticles stuck on the mucosal surface (M%/cm²) after 2 h of contact, number of theoretical nanoparticles attached onto 1 cm² mucosal surface and number of theoretical nanoparticles layers formed onto 1 cm² mucosal surface

	CS-P-NPs	CSNAC-P-NPs	CSGSH-P-NPs	GCS-P-NPs	GCSNAC-P-NPs	GCSGSH-P-NPs
M%/cm²	20.1 ± 9.9	44.9 ± 16.5	38.4 ± 20.3	19.4 ± 3.2	15.8 ± 9.8	76.3 ± 19.8
Number of NPs attached to mucosa(x 10⁹)	50	32.3	28	472	970	4118
Number of NPs layers formed onto the mucosal surface (1 cm²)	5	118	101	349	849	3931

Abstract

The aim of the present work was to evaluate the mucoadhesive properties of poly(isobutyl cyanoacrylate) (PIBCA) nanoparticles (NPs) coated with Low Molecular Weight (LMW) chitosan (CS)- and glycol chitosan (GCS)-based thiomers as well as with the corresponding LMW unmodified polysaccharides. For this purpose, all the CS- and GCS-based thiomers were prepared under simple and mild conditions starting from the LMW unmodified polymers CS and GCS. The resulting NPs were of spherical shape with diameters ranging from 400 to 600 nm and 187 to 309 nm, for CS- and GCS-based NPs, respectively. The mucoadhesive characteristics of these core shell NPs were studied in Ussing chambers measuring the percentage of NPs stuck on the mucosal of fresh intestinal tissue after 2 h of incubation. Moreover, incubation of nanoparticle formulations with the intestinal tissue induced changes in transmucosal electrical resistance which were measured to gain information into the opening of tight junctions and to control the integrity of the mucosa. Thus, it was found that PIBCA NPs coated with the GCS–Glutathione conjugate (GCGPIBCA NPs) possessed the most favorable mucoadhesive performances. Moreover, both GCGPIBCA- and GCS-*N*-acetyl-cysteine (GCNPIBCA)-core-shell NPs might induced an enlargement of the epithelial cell tight junctions. In conclusion, coating of PIBCA NPs with GCS-based thiomers may be useful for improving the mucoadhesive and permeation properties of these nanocarriers.

Keywords: Mucoadhesion, Thiomers, Ussing chambers, Chitosan, Glycol Chitosan